



Effect of HCO_3^- concentration in groundwater on TiO_2 photocatalytic water purification

Nobuaki Negishi^{a,*}, Yukari Miyazaki^a, Shigekazu Kato^b, Yingnan Yang^c

^a Environmental Management Research Institute, National Institute of Advanced Industrial Science and Technology (AIST), 16-1 Onogawa, Tsukuba 305-8569, Japan

^b Photocatalytic Materials Incorporated, 1-10 Sakurayama-cho, Showa-ku, Nagoya 466-0044, Japan

^c Graduate School of Life and Environmental Science, University of Tsukuba, 1-1-1 Tennodai, Tsukuba, Ibaraki 305-0006, Japan



ARTICLE INFO

Keywords:
 TiO_2 ceramic photocatalyst
 Water purification
 Mineral water
 Bicarbonate ion
 Formic acid

ABSTRACT

Evaluation of the effects of major components of groundwater systems on photocatalytic activity is essential for the development of commercial photocatalytic water purification systems. In this work, we have probed the effects of bicarbonate ion (HCO_3^-) on the photocatalytic activity of a TiO_2 ceramic photocatalyst. Two brands of mineral water, Evian and Contrex, which contain high concentrations of alkaline earth metal ions Mg^{2+} and Ca^{2+} , were used as models for groundwater. The degradation rate of formic acid was used as an index of photocatalytic activity. The rate of HCO_3^- degradation and changes in the type and concentration of the HCO_3^- counterion with the progress of photocatalytic reaction were also observed. After the completion of 15 cycles of 8 h of photocatalytic reaction (total run time 120 h), the surface of the photocatalyst and precipitates formed on it were analyzed by means of X-ray diffraction analysis, Raman spectrometry, scanning electron microscopy, and energy dispersive X-ray spectrometry. We found that the photocatalytic activity was reduced with increasing HCO_3^- concentration, irrespective of the type of counterion present. In addition, photocatalytic activity remained unchanged despite an increase in accumulation of the precipitate, which we identified as CaCO_3 , on the photocatalyst surface with the progress of experimental cycles. We also observed that the concentration of formic acid and HCO_3^- were decreased with photocatalysis when Ca^{2+} was a counterion, however, no effect in presence of other metal ions, Na^+ , K^+ or Mg^{2+} , was observed. These results show that bicarbonate ion was involved in the photocatalytic reaction when Ca^{2+} was the counterion, and as a result, the photocatalytic degradation rate of formic acid was decreased and CaCO_3 precipitate was formed.

1. Introduction

Clean drinking water problem is a serious concern in many developing countries, and the groundwater like well water and spring water, which is generally considered safe, is also contaminated by microbes, and pesticides etc. [1–7], and therefore, there is an urgent need to develop efficient water treatment technology. The major bottleneck of using the water treatment technology in these countries is its high initial and running cost. We envisage that the photocatalytic technology for water treatment would provide these developing countries with the cheap and safe water purification system as the energy source for activation of photocatalyst is only sunlight. Various photocatalytic technologies are already available with applications in air purification, production of self-sterilizing materials, and sterilization of surgical instruments, and as per literature reports, enough research work has also been carried out related to the purification of water by photocatalysis,

which is not yet commercialized. Photocatalysis Industry Association of Japan (PIAJ) gives the PIAJ approval to the photocatalyst products that meet the established performance standards. Surprisingly, PIAJ has not yet certified any photocatalyst product for water purification out of 105 finished products (self-cleaning = 72, air purification = 11, anti-virus = 2, and anti-bacteria = 20) [8], which immediately demands to find the bottleneck in the practical use of photocatalytic water purification and solve it. Some research groups expect the presence of total dissolved solids (TDS) such as minerals, could limit the use of photocatalytic water purification technique, however the work done up till now in this direction does not confirm this [9].

The major ionic components of groundwater are the cations Ca^{2+} , Mg^{2+} , Na^+ , and K^+ and the anions SO_4^{2-} , HCO_3^- , CO_3^{2-} , and SiO_3^{2-} [10,11]. The effect of HCO_3^- ions on photocatalysis has been examined in several studies using NaHCO_3 [12–14]. As a result, it is clarified that HCO_3^- ion coordinated with monovalent ions such as Na^+ as its

* Corresponding author.

E-mail address: n-negishi@aist.go.jp (N. Negishi).

counterion was badly influenced the photocatalysis [12]. On the other hand, Ca^{2+} , a bivalent ion, is one of the major components in groundwater [11], however, nobody studied the effect of bivalent ion against photocatalysis. Therefore we wished to study the photocatalytic reactions in presence of Ca^{2+} ions prior to the development of any commercial photocatalytic water purification process.

In this manuscript, we have examined the effect of HCO_3^- ion on photocatalysis in presence of Mg^{2+} or Ca^{2+} as its counterion in place of Na^+ . $\text{Ca}(\text{HCO}_3)_2$ and $\text{Mg}(\text{HCO}_3)_2$ are commercially not available as they are unstable under atmospheric condition, so we prepared their aqueous solutions prior to every photocatalytic experiment. In contrast, NaHCO_3 is commercially available and is stable in aqueous solution. According to some literature reports, NaHCO_3 changes to Na_2CO_3 by photocatalysis and likewise, the conversion of $\text{Mg}(\text{HCO}_3)_2$ and $\text{Ca}(\text{HCO}_3)_2$ to MgCO_3 and CaCO_3 respectively, is also expected. Na_2CO_3 is water soluble whereas CaCO_3 and MgCO_3 have low solubility in water, and therefore, their precipitation onto the surface of the photocatalyst needs to be confirmed. It is also important to probe the impact of precipitated compounds on the photocatalytic activity for commercialization, long-term use and maintenance of such photocatalytic water purification systems.

Some commercial mineral water bottles contain $\text{Ca}(\text{HCO}_3)_2$ and/or $\text{Mg}(\text{HCO}_3)_2$, and high concentration of HCO_3^- ions, which is suitable to evaluate the photocatalytic activity since the initial concentration of HCO_3^- is almost equal regardless of the make of bottles. In this study, we also prepared and used two types of groundwater-simulated water (aqueous solutions of $\text{Mg}(\text{HCO}_3)_2$ and $\text{Ca}(\text{HCO}_3)_2$), in addition to our commercially available mineral water, Evian and Contrex.

2. Experimental

2.1. Construction of a closed photocatalytic water purification system

We constructed a closed photocatalytic water purification system, which comprised of two lines, wherein each line contained a 500-mL water reservoir, a solenoid-driven metering pump (PW-100, Tacmina, Osaka, Japan), a Pyrex glass tube ($300 \text{ mL} \times 10 \text{ mm}$ (I.D.), thickness = 1 mm) packed with a TiO_2 ceramic photocatalyst monolith (PSF-01, Photocatalytic Materials Inc., Nagoya, Japan), and a 15 W black-light bulb (Toshiba, Tokyo, Japan) (Fig. 1). The UV intensity ($\lambda = 365 \text{ nm}$) of the black-light bulb after passing through 1 mm of Pyrex glass was around 2.5 mW/cm^2 , as measured by a UV power meter (C9356-1, Hamamatsu Photonics, Hamamatsu, Japan). PSF-01 is a porous TiO_2 ceramic photocatalyst comprising of anatase, brookite, and rutile crystal forms; is a monolith with a length of 2–8 mm and a thickness of 1 mm, and approximately 26 g of it was packed in the Pyrex tube.

2.2. Preparation of bicarbonate solutions

The aqueous solutions of $\text{Mg}(\text{HCO}_3)_2$ and $\text{Ca}(\text{HCO}_3)_2$ were prepared from their respective $\text{Mg}(\text{OH})_2$ and $\text{Ca}(\text{OH})_2$ white powders (Wako Chemicals, Tokyo, Japan). 10 g of $\text{Mg}(\text{OH})_2$ or $\text{Ca}(\text{OH})_2$ was poured in a flask containing 10 L water, and was strongly stirred to obtain a slurry of $\text{Mg}(\text{OH})_2$ and $\text{Ca}(\text{OH})_2$. CO_2 gas was continuously and excessively purged into the slurry for few hours. The slurry became transparent and saturated aqueous solutions of $\text{Mg}(\text{HCO}_3)_2$ and $\text{Ca}(\text{HCO}_3)_2$ were obtained after the removal of unreacted hydroxides by means of paper filtration [15]. $\text{Ca}(\text{HCO}_3)_2$ is unstable and gradually deteriorates with time, therefore, the concentration of HCO_3^- ions was checked prior to every experiment using a spectroscopic method as reported by Mishima et al. [16]. The aqueous solutions of NaHCO_3 and KHCO_3 were prepared by dissolving their respective granular powder (Wako Chemicals, Tokyo, Japan) in water. The concentration of cations in these four solutions was measured by using an ion chromatography (IC-2010; Tosoh Co., Tokyo, Japan), while that of bicarbonate ions is calculated from the

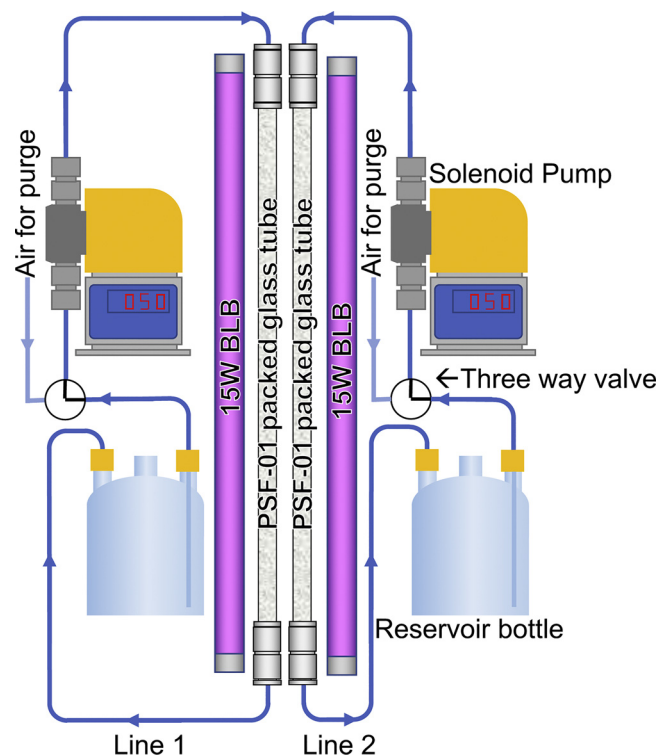


Fig. 1. Schematic diagram of the photocatalytic water purification system. BLB (Blacklight bulb), PSF-01 (TiO_2 ceramic photocatalyst).

ratio of absorption intensities, which changes with bicarbonate ion concentration, in the UV-vis absorption spectra of bromocresol green solution (0.04% w/v) (Wako Chemicals, Tokyo, Japan) between longer and shorter absorption peaks. In order to measure the bicarbonate ion concentration in mineral water, a calibration curve of HCO_3^- concentration was prepared, wherein a stock solution of aq. NaHCO_3 (500 mg/L) was made and diluted to 100, 200, 300, 400 and 450 mg/L solutions. Next, $1.0 \times 10^{-4} \text{ M HCl}$ solution was prepared from 0.1 M HCl solution (Wako Chemicals, Tokyo, Japan). A solution to detect bicarbonate ions was prepared by mixing 10 mL of aq. HCl solution ($1 \times 10^{-4} \text{ M}$) and 0.38 mL of the bromocresol green solution in a transparent 30 mL polyethylene terephthalate bottle. To this solution, an aliquot (100 μL) of each concentration of NaHCO_3 solutions was added, and the absorbance was observed after mixing for five minutes. Mishima et al. measured the changes in the ratio of the maximum absorption intensity of the spectra of twin peaks at 445 and 615 nm by UV-vis spectrometer, whereas, we measured the changes in absorbance of the sample solutions at 470 nm and 615 nm by portable multi-parameter water analyzer (A9000; Kyoritsu Chemical-Check Lab. Corp., Tokyo, Japan). The results obtained from both the methods corroborated well. We prepared the calibration curve employing the portable-parameter water analyzer, and was used to detect the concentration of HCO_3^- ions in water.

2.3. Photocatalytic reaction

In this study we used an aqueous solution of formic acid (1 mM). The photocatalytic reaction of TiO_2 is described in Eqs. (1) and (2). Formic acid reacts with $\cdot\text{OH}$ derived from (2) and is photodecomposed to CO_2 and H_2O via first order reaction with no side reactions (Eqs. (3) and (4)), making it a suitable choice to examine the photocatalytic activity.





The photocatalytic degradation rate of aqueous solution of formic acid (1 mM) by photocatalysis under UV irradiation for 8 h was obtained from the photocatalytic reaction system, shown in Fig. 1. This photocatalytic reaction was repeated 15 times to observe the changes in the photocatalytic degradation rate with an increase in number of reaction cycles. Before starting the photocatalytic reaction, the aqueous solution of formic acid (1 mM) was circulated in the photocatalytic system for 3 times, and the average rate constant of photocatalytic degradation of formic acid (k_{MQ}) was obtained, which was used as the standard rate constant for photodegradation of formic acid. The photocatalytic degradation rate of formic acid in solutions containing total dissolved substances (k_x , where $x = \text{Ev. (Evian), Cont. (Contrex), Na, K, Mg or Ca}$) was normalized by dividing with the standard rate constant. Similarly, the decrease in rate of HCO_3^- ions in water was obtained from the photocatalytic reaction system and the changes in the degradation rate of HCO_3^- with number of experimental cycles was observed. In order to confirm the photocatalysis of HCO_3^- ions in case of Evian and Contrex system, we have also performed the experiment in dark i.e., without UV irradiation.

After every 8 h photocatalytic reaction cycle, the system underwent maintenance wherein, the photocatalytic water circulation system was drained by blowing air, followed by the circulation of pure water for 10 min, which was drained again by air blow. The system was then dried overnight under an air flow and UV irradiation to ensure the elimination of any residual organic materials on the surface of PSF-01. A series of 8-hour circulation process followed by maintenance process is counted as one experimental protocol.

The changes in the concentrations of formic acid and cations within every 8 h reaction cycle were observed by using an ion chromatography IC-2001 and IC 2010 (Tosoh Co., Tokyo, Japan) respectively, while the concentration changes in HCO_3^- ions were observed by using the absorbance method described in Section 2.2. The samples were taken after every hour for measuring ion chromatography and HCO_3^- ions absorbance in 8 h circulation. After the completion of 15 experimental cycles, the photocatalyst monolith was taken out from the Pyrex tube and subjected to X-ray diffraction (XRD) analysis (D2 Phaser; Bruker, Germany) and Raman spectrometry (NRS-4500; JASCO, Tokyo, Japan) to determine the crystal structures, and to scanning electron microscopy/energy dispersive X-ray spectrometry (SEM/EDX) (JSM-6010LA; JEOL, Tokyo, Japan) for morphology and elemental composition of any precipitate that had formed. EDX analysis was performed in an auto mode.

To study the effect of HCO_3^- ion concentration on photocatalytic activity, the photocatalytic degradation rate of formic acid in various concentrations of aqueous solutions of NaHCO_3 , KHCO_3 , $\text{Mg}(\text{HCO}_3)_2$, or $\text{Ca}(\text{HCO}_3)_2$ was determined for 8 h reaction cycle. After every 8 h reaction cycle, the photocatalytic system was flushed with 0.1 N HCl solution to prevent any precipitation affecting the next experiment on PSF-01 surface. Deionized water was then passed through the system for at least 1 h to remove residual Cl^- ions, and residual organic materials were removed by drying the PSF-01 overnight under an air flow and UV irradiation.

3. Results and discussion

3.1. Photocatalytic reactions

Although the concentration of HCO_3^- in Evian and Contrex is not mentioned on the products' labels, the average concentrations obtained by means of colorimetry using bromocresol green were found to be 295 mg/L and 305 mg/L, respectively.

First, we observed the changes in the photocatalytic decomposition

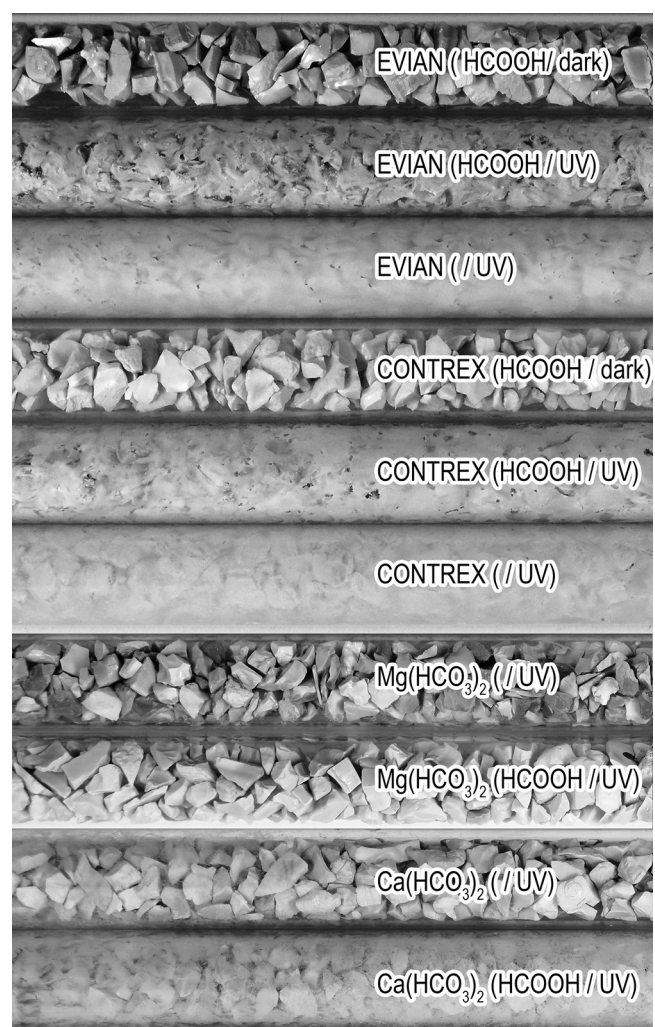


Fig. 2. Representative photographs showing the appearance of the PSF-01-packed Pyrex tube after 15 experimental cycles (total run time: 120 h).

rate of formic acid in both the mineral water samples for 15 experimental cycles of 8 h each (total run time: 120 h). Three experimental conditions were followed: with formic acid in dark and under UV irradiation, and under UV irradiation without formic acid. When the experiment was conducted under UV irradiation with or without formic acid, the formation of white precipitate was increased with an increase in number of experimental cycles, and after 15 cycles, a white scale was accumulated on the surface of photocatalyst monolith and inside the wall of Pyrex tube (Fig. 2). We could not visually observe the precipitate on PSF-01 surface when the experiment was conducted in dark.

Fig. 3A and B show an exponential decay of formic acid in Evian and Contrex systems over 15 experimental cycles and the rate constant (k) for the photocatalytic degradation of formic acid was calculated by fitting this decay curve. Fig. 3C shows the plot of these rate constants normalized by the standard rate constant for the photocatalytic degradation of formic acid in pure water (k_{MQ}). Despite the accumulation of precipitate on the surface of the photocatalyst monolith and inside wall of Pyrex tube as shown in Fig. 2, only a small decrease in the photocatalytic activity was observed.

Similarly, we then observed changes in HCO_3^- ion concentration in Evian and Contrex systems for 15 experimental cycles of 8 h each under same experimental conditions. When the experiment was conducted in dark in presence of formic acid, the degradation rate of HCO_3^- ions in both the mineral water systems decreased with increasing experimental cycles and finally approached zero as shown in Fig. 4. On the other

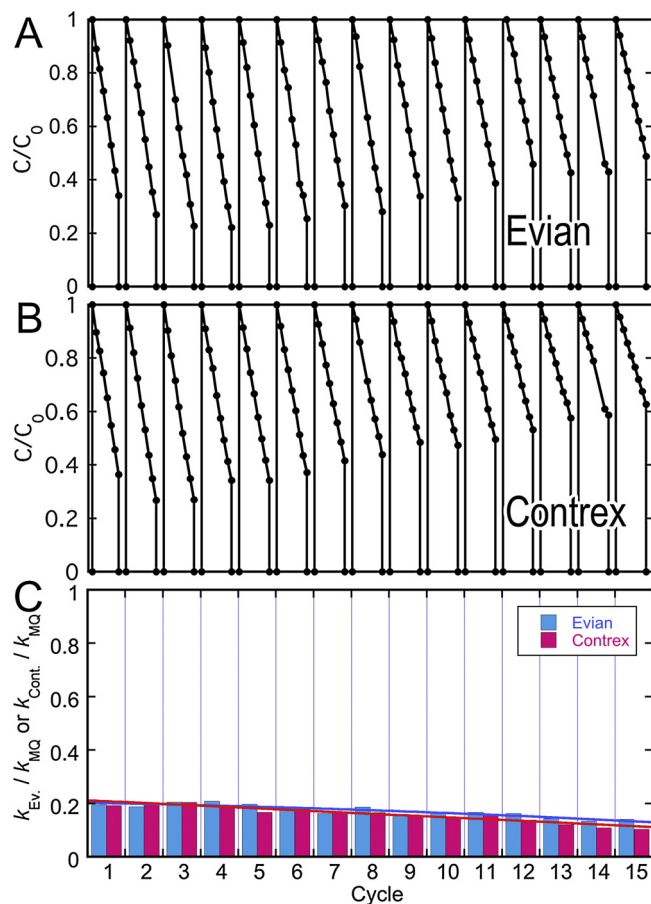


Fig. 3. Decay curve of formic acid in Evian [A] or Contrex [B] system for 15 repeat experimental cycles, [C] Rate constant for the photocatalytic degradation of formic acid in Evian ($k_{Ev.}$) or Contrex ($k_{Cont.}$) normalized by the rate constant for the photocatalytic degradation of formic acid in pure water (k_{MQ}).

hand, high degradation rate of HCO_3^- ion was observed for both the mineral water systems with the progress of experimental cycles under UV irradiation with or without formic acid. The rate constants remain unchanged for Evian system, while they show an increase in case of Contrex system. The reason for a decrease in the degradation rate of HCO_3^- ions under dark condition was speculated as catalytic effect

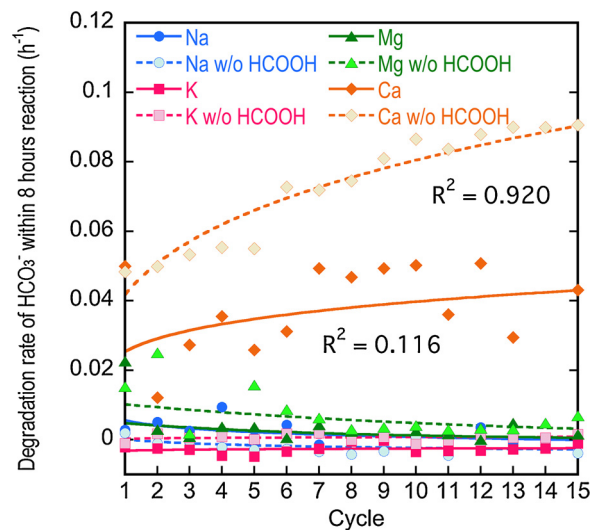


Fig. 5. Changes in the degradation rate of HCO_3^- in NaHCO_3 , KHCO_3 , $\text{Mg}(\text{HCO}_3)_2$, and $\text{Ca}(\text{HCO}_3)_2$ solutions circulated systems for 15 experimental cycles.

[17], implying that $\text{Ca}(\text{HCO}_3)_2$ was converted to CaCO_3 which was adsorbed onto TiO_2 surface when brought in contact with fresh TiO_2 surface. Catalytic (not photocatalytic) effect was reduced by coating TiO_2 surface with a thin layer of CaCO_3 , resulting in a decrease in the degradation rate of $\text{Ca}(\text{HCO}_3)_2$ with increasing experimental cycles.

Since these commercial mineral water systems include various kinds of components, we should mind that it is possible that one or more of these components were involved in the observed changes of bicarbonate ion concentration. To address this issue, we prepared two simple bivalent metal ion bicarbonate solutions, $\text{Mg}(\text{HCO}_3)_2$ and $\text{Ca}(\text{HCO}_3)_2$ and circulated these solutions through the photocatalytic water purification system. In order to compare the HCO_3^- efficiency against photocatalysis in bivalent cation systems, we performed same experiments using NaHCO_3 and KHCO_3 solutions.

Fig. 5 shows the changes in the HCO_3^- degradation rate when the above mentioned four simulated water systems were circulated through the photocatalytic water purification system with formic acid under UV irradiation for 15 experimental cycles. Only $\text{Ca}(\text{HCO}_3)_2$ solution circulated system resulted in a white precipitate after 15 cycles as shown in Fig. 2. When $\text{Ca}(\text{HCO}_3)_2$ solution was circulated through the system,

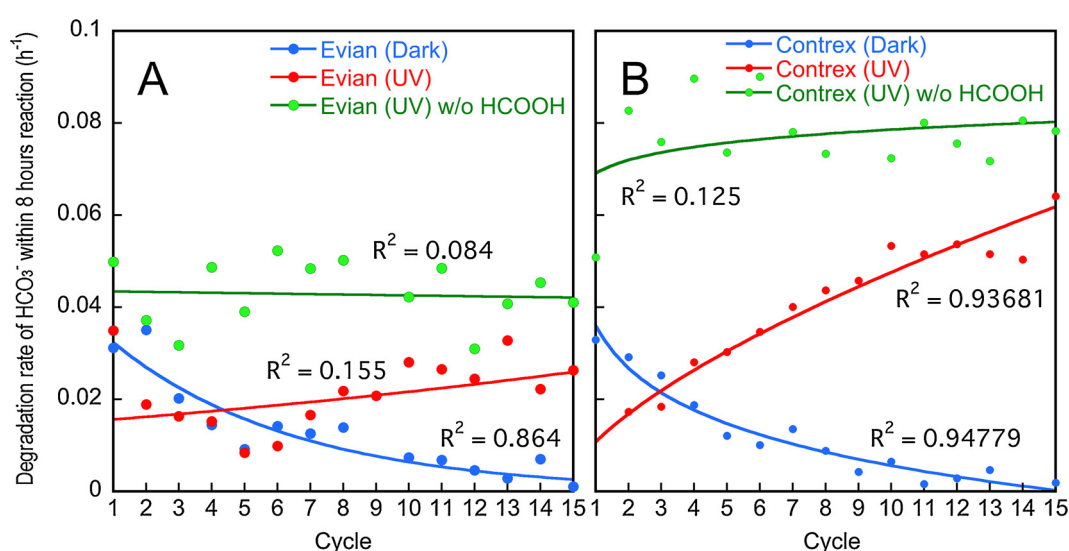


Fig. 4. Changes in the rate of HCO_3^- degradation for 15 repeat experimental cycles in Evian and Contrex circulated systems.

Table 1
Major ion concentrations in ground waters and simulated waters.

	Na ⁺	K ⁺	Mg ²⁺	Ca ²⁺	HCO ₃ ⁻	SO ₄ ²⁻
Evian	6.3 (7)	1.9 (1)	22.3 (26)	64.5 (80)	294.6 (357)	8.8 (13)
Contrex	7.9 (9.4)	1.5 (2.8)	79.0 (74.8)	542.8 (468)	304.9 (372) (1121)	1230
NaHCO ₃	198	–	–	–	457	–
KHCO ₃	–	284	–	–	386	–
Ca(HCO ₃) ₂	–	–	71	–	264	–
Mg(HCO ₃) ₂	–	–	–	120	247	–

Unit: mg/L.

Ion concentrations as stated on the products' label are in parentheses.

the decrease trend in the rate of degradation of HCO₃⁻ ions was similar to that in Contrex system (Figs. 4 and 5). This similarity is dependent on the concentrations of Ca²⁺ and HCO₃⁻ in both the solution systems. In contrast, the degradation rate of HCO₃⁻ ions did not show any significant change with the progress of experiment in case of solutions of NaHCO₃, KHCO₃ and Mg(HCO₃)₂ as clearly evident from Fig. 5. These results show that HCO₃⁻ ions react by photocatalysis when only Ca²⁺ ions were circulated through the system.

These results clearly prove that the type of counterions present is an important factor for the photocatalytic oxidation of organic compounds. Table 1 shows the concentrations of several ionic species in Evian, Contrex, and our four simulated water systems. The cationic components that are able to coordinate with HCO₃⁻ ions in Evian and Contrex were Na⁺, K⁺, Mg²⁺, and Ca²⁺. In our experiments, a precipitate was observed only when water containing Ca²⁺ was circulated through the system.

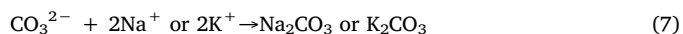
If we assume that Ca²⁺ is the only cause of precipitation, it is expected that the concentration of Ca²⁺ in water will decrease with increasing photocatalytic reaction time. Therefore, we monitored the changes of cation concentration in Evian and Contrex systems for 15 experimental cycles under same three experimental conditions (Fig. 6A–F). The concentration of Ca²⁺ under dark condition was only slightly decreased or not with the progress the experimental cycles (Fig. 6A, D). In contrast, marked decrease in Ca²⁺ concentration was observed when the water systems without formic acid were circulated through the system under UV irradiation (Fig. 6C, F). In case of a single cation system, only Ca(HCO₃)₂ solution system revealed a decrease of Ca²⁺ concentration whereas other cations did not show any decrease of respective cation with increasing number of experimental cycles (Fig. 6G). In conclusion, under all experimental conditions and water systems, the concentrations of Na⁺, K⁺, and Mg²⁺ remained constant indicating that the precipitate was derived only from Ca²⁺.

We hypothesized that the four bicarbonate salts would convert to their respective carbonate salts via photocatalysis in the following way:

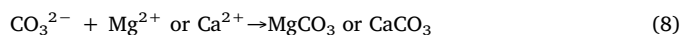


·OH and OH_{ad}⁻ were generated from Eq. (2). HCO₃⁻ on reaction with ·OH generates ·CO₃⁻ as shown in Eq. (5) [18]. On the other hand, ·CO₃⁻ is expected to react with OH_{ad}⁻ and generate CO₃²⁻ as shown in Eq. (6). The motivation behind this hypothesis of reaction sequence comes from the similar equations described by Wang et al. [19], where they explained that adsorbed SO₃²⁻ onto TiO₂ surface reacted with ·CO₃⁻ to form CO₃²⁻ and ·SO₃⁻.

When the counterion of HCO₃⁻ is Na⁺ or K⁺:



When the counterion of HCO₃⁻ is Mg²⁺ or Ca²⁺:



It is important to note that there were no changes in HCO₃⁻ concentration in the water systems containing Na⁺, K⁺, and Mg²⁺ even after 15 experimental cycles, as shown in Fig. 5. That is, the reactions shown in Eq. (7) did not apparently occur, and the reaction shown in Eq. (8) occurred only when the water containing Ca²⁺ was circulated through the system. Thus, we estimate that the substance precipitating on the surface of the catalyst was only CaCO₃ by Eq. (8), regardless of the composition ratio of groundwater (Ca²⁺, Mg²⁺, Na⁺, etc.). It is likely that Na₂CO₃, K₂CO₃, and MgCO₃ did not precipitate because the solubility of these compounds would be higher than that of CaCO₃. On the other hand, the concentration of HCO₃⁻ remained unchanged with increasing experimental cycles, showing that photocatalytic reaction of HCO₃⁻ in the water systems containing Na⁺, K⁺, and Mg²⁺ did not occur, except for that containing Ca²⁺. The mechanism of the stability of HCO₃⁻ concentration under photocatalysis, except for Ca²⁺ contained system, is related with the equilibrium between carbonate and bicarbonate in aqueous phase, and is described in details in the Section 3.3.

3.2. Characterization of the precipitate

To characterize the precipitate and confirm that it was certainly CaCO₃, we studied its morphology and elemental composition by means of SEM/EDX, and we determined its crystal structure by means of XRD analysis and Raman spectroscopy. Fig. 7 shows SEM and EDX images of PSF-01 surface after 15 experimental cycles. The surface of fresh photocatalyst was smooth and contained mainly Ti and O, and a small amount of C, which could be attributed to some organic contamination (Fig. 7A). After circulating Evian in presence of formic acid under dark condition, the surface of PSF-01 was largely unchanged as compared to fresh photocatalyst, and the same elemental composition was observed (Fig. S1). On the other hand, when Evian system was circulated in presence of formic acid under UV irradiation, some kind of crystals were formed on the surface of PSF-01, which consisted of C, O, and Ca (Fig. S2). Fig. 7B shows the surface of PSF-01 after circulation of Evian without formic acid under UV irradiation; EDX analysis revealed that same elemental composition with and without formic acid under UV irradiation (Figs. 7B and S2). The elements in this precipitate were C, O, and Ca (Figs. 7B and S2) and this may indicate the presence of calcium carbonate. We also found that a small amount of calcium carbonate was deposited on PSF-01 circulated with Contrex in presence of formic acid in the dark (Fig. S3), and this formation of calcium carbonate was different to what was observed after circulation of Evian with formic acid in the dark (Fig. S3). Fig. 7C shows the surface of PSF-01 after circulation of Contrex without formic acid under UV irradiation; almost the entire surface was covered with calcium carbonate as evident from its elemental analysis, which showed the presence of C, O and Ca. Strontium (Sr) was detected on the surface of photocatalyst in Contrex system under UV irradiation irrespective of presence of formic acid (Figs. 7C and S4). Contrex has a relatively high concentration of Sr along with other minor elements, and the result of the EDX analysis revealed that the precipitate formed during these experiments comprised a mixture crystal of Ca and Sr atoms. On the other hand, it was difficult to observe Sulfur (S) on the surface of the photocatalyst in spite of being present in higher concentration as SO₄²⁻ in Contrex system. This could be because of the fact that sulfate ions are water soluble and did not get deposited on TiO₂ and/or calcium carbonate surface as they were washed away during the maintenance process in each experimental cycle. Indeed, this result shows that SO₄²⁻ was not trapped to the calcium carbonate surface as no change in SO₄²⁻ concentration was observed in Contrex after photocatalysis for 8 h as shown in Fig. S5.

Figs. S6 and S7 illustrate the surface of PSF-01 for Mg(HCO₃)₂ solution without and with formic acid system under UV irradiation, respectively after 15 experimental cycles. SEM images show that no precipitate was formed on the surface of PSF-01 irrespective of the presence or absence of formic acid. EDX analysis revealed the presence

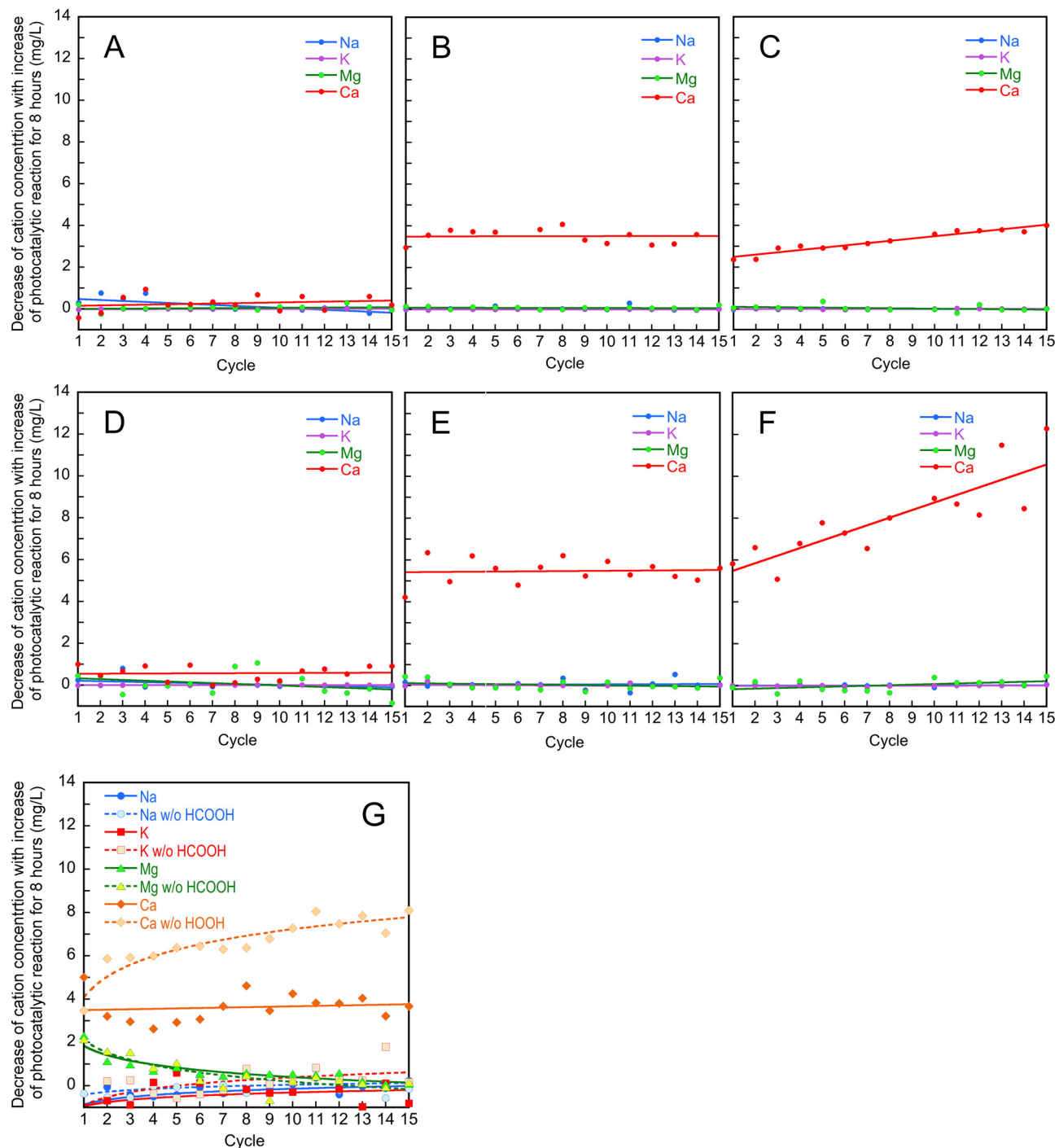


Fig. 6. Changes in concentration of cations (Na^+ , K^+ , Mg^{2+} , and Ca^{2+}) with increasing cycle number. [A] Evian with formic acid in the dark, [B] Evian with formic acid under UV irradiation, [C] Evian without formic acid under UV irradiation, [D] Contrex with formic acid in the dark, [E] Contrex with formic acid under UV irradiation, [F] Contrex without formic acid under UV irradiation, and [G]: NaHCO_3 , KHCO_3 , $\text{Mg}(\text{HCO}_3)_2$ and $\text{Ca}(\text{HCO}_3)_2$ with formic acid under UV irradiation.

of Ti, O, and C, but not Mg.

Figs. 7D and S8 show the surface of PSF-01 after 15 experimental cycles for $\text{Ca}(\text{HCO}_3)_2$ solution without and with formic acid under UV irradiation, respectively. SEM images show that a precipitate was formed on PSF-01 (Figs. 7D and S8). EDX analysis revealed that the elements on PSF-01 surface were Ti, O, C, and Ca, and we concluded that the precipitate was CaCO_3 .

Next, we examined the precipitate on PSF-01 by means of XRD and Raman spectroscopy. The XRD spectrum of the fresh photocatalyst revealed that it is a mixture of anatase, rutile, and brookite crystal forms (Fig. S9). XRD spectrum of the precipitate on PSF-01 surface after 15

experimental cycles for Evian or Contrex, independent of the experimental conditions (UV irradiation with/without formic acid) revealed the aragonite crystal form (Fig. 8A, B). XRD spectrum of PSF-01 surface after 15 experimental cycles under UV irradiation for $\text{Mg}(\text{HCO}_3)_2$ solution was similar to that for fresh photocatalyst regardless of the presence of formic acid (Fig. 8C), which corroborates with the finding that no precipitate was formed when $\text{Mg}(\text{HCO}_3)_2$ solution was circulated through the system. Thus, we confirmed that any precipitate derived from Mg^{2+} did not accumulate on the surface of PSF-01. On the other hand, XRD analysis of PSF-01 surface for $\text{Ca}(\text{HCO}_3)_2$ solution after 15 experimental cycles under UV irradiation revealed the presence of

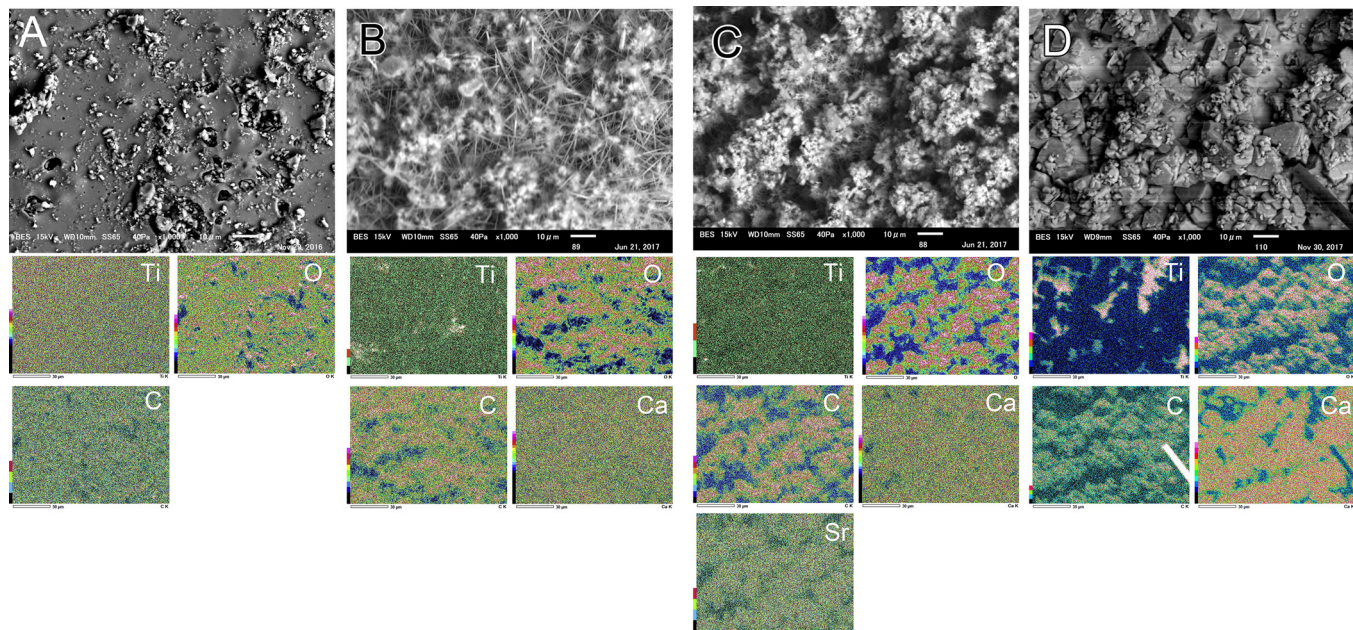


Fig. 7. Scanning electron microscopy and energy dispersive X-ray spectrometry images of PSF-01 surface after 15 experimental cycles. [A] Fresh PSF-01 surface, [B] Evian without formic acid system under UV irradiation, [C] Contrex without formic acid system under UV irradiation, and [D] $\text{Ca}(\text{HCO}_3)_2$ solution without formic acid system under UV irradiation.

calcite crystal form irrespective of the presence of formic acid, which is different from the aragonite crystal in the Contrex system. It is known that the formation of aragonite requires coexistence of inorganic substance in the system when crystal is being formed, especially ionic species with radii larger than that of Ca, such as Sr [20,21], therefore, aragonite was formed in Evian and Contrex systems. However, $\text{Ca}(\text{HCO}_3)_2$ solution system was a single component phase and therefore only calcite crystals were formed instead of aragonite.

Fig. 9 shows Raman spectra of PSF-01 surface for Evian, Contrex, $\text{Mg}(\text{HCO}_3)_2$ solution and $\text{Ca}(\text{HCO}_3)_2$ solution system after 15 experimental cycles under UV irradiation in absence of formic acid. Fig. S10 shows Raman spectra of the fresh PSF-01 surface revealing a mixture of the anatase, rutile, and brookite crystal forms, which is consistent with the results of the XRD analysis. The characteristic Raman peaks for calcite and aragonite are at around 280 cm^{-1} 205 cm^{-1} , respectively. Evian and Contrex systems exhibited Raman peaks at 205 cm^{-1} (Fig. 9A, B), which is attributed to aragonite, in addition, the crystals on PSF-01 were acicular (Figs. 7B, S2 and S3). Only $(\text{Ca}_{0.96}\text{Sr}_{0.02})_{\Sigma=0.98}\text{CO}_3$ corresponds to aragonite containing Sr and forming acicular crystals [22].

Fig. 9C and D show Raman spectra of PSF-01 for $\text{Mg}(\text{HCO}_3)_2$ and $\text{Ca}(\text{HCO}_3)_2$ solution systems, respectively, after 15 experimental cycles. In case of $\text{Mg}(\text{HCO}_3)_2$ solution, the Raman spectrum was comparable with that of fresh photocatalyst, which is consistent with the XRD results. However, when $\text{Ca}(\text{HCO}_3)_2$ solution was used, the Raman spectrum indicated the existence of calcite, which is in accordance with the XRD analysis (Fig. 9D). When $\text{Ca}(\text{HCO}_3)_2$ solution was used, no metal cations larger than Ca^{2+} were present to trigger aragonite formation on the surface of PSF-01; indicating only calcite was formed.

We also determined the elemental ratios in the precipitates by means of EDX analysis after Evian or Contrex were circulated through the system (Table 2). When Evian was circulated under dark conditions, the amount of calcium carbonate deposited on PSF-01 was very small. While in case of Contrex, PSF-01 was covered with calcium carbonate (i.e., aragonite), and as a result only a small amount of Ti was detected for all experimental conditions. We then focused on the ratio of C, O, Ca, and Sr in the Contrex system. wherein, the ratio of these elements in the precipitate was almost same as that for Evian system ($\text{Ca:C:O} =$

1:1:3) (Table 2) confirming that the precipitate on PSF-01 was of CaCO_3 . The elemental ratio of Ca to Sr was approximately 1/100 when Contrex was circulated through the system under UV irradiation with or without formic acid (Table 2). The composition of aragonite including Sr is $(\text{Ca}_{0.96}\text{Sr}_{0.02})_{\Sigma=0.98}\text{CO}_3$, where the ratio of Ca to Sr is around 50:1, therefore, it is considered that the crystal ratio of aragonite deposited on PSF-01 having simple aragonite (CaCO_3) and Sr containing aragonite ($\text{Ca}_{0.96}\text{Sr}_{0.02})_{\Sigma=0.98}\text{CO}_3$ was around 1:1. When Evian was circulated in the system, the elemental ratio of Sr was relatively small indicating that the aragonite accumulated on PSF-01 surface was mainly CaCO_3 and not $(\text{Ca}_{0.96}\text{Sr}_{0.02})_{\Sigma=0.98}\text{CO}_3$.

It is clear that calcium carbonate was deposited on PSF-01 surface when the water system contained calcium bicarbonate. However, we did not find a correlation between the amount of accumulated compound and its photocatalytic activity i.e., accumulation of precipitate did not induce a decrease in the photocatalytic activity (Figs. 2 and 3). We hypothesize that the photocatalytic activity remained unchanged even with the accumulation of precipitate on PSF-01 due to the specific composition of the precipitate. The precipitate contained only calcium carbonate having no absorption band within UV-A range ($\lambda = 365 \text{ nm}$), which is the excitation wavelength for TiO_2 photocatalyst. In addition, the accumulation of calcium carbonate onto TiO_2 surface on these experiments was very rough (Fig. 7B, C and E), so we expected that the precipitate did not prevent the contact between formic acid molecules and PSF-01.

Although the precipitate did not inhibit the photocatalysis, the formation of too much precipitate would block the flow channel, which needs to be removed for its real-world application.

3.3. Effect of HCO_3^- on photocatalytic activity

The effect of HCO_3^- on the photocatalytic activity has been examined using NaHCO_3 solution by other groups [12,13,23,24], however, no studies have been conducted using $\text{Mg}(\text{HCO}_3)_2$ and $\text{Ca}(\text{HCO}_3)_2$ solutions. In this regard, we probed the underlying mechanism of the effect of HCO_3^- on photocatalytic activity and examined how different counterions of HCO_3^- affected the photocatalytic degradation rate of organic compound by using four different bicarbonate solutions

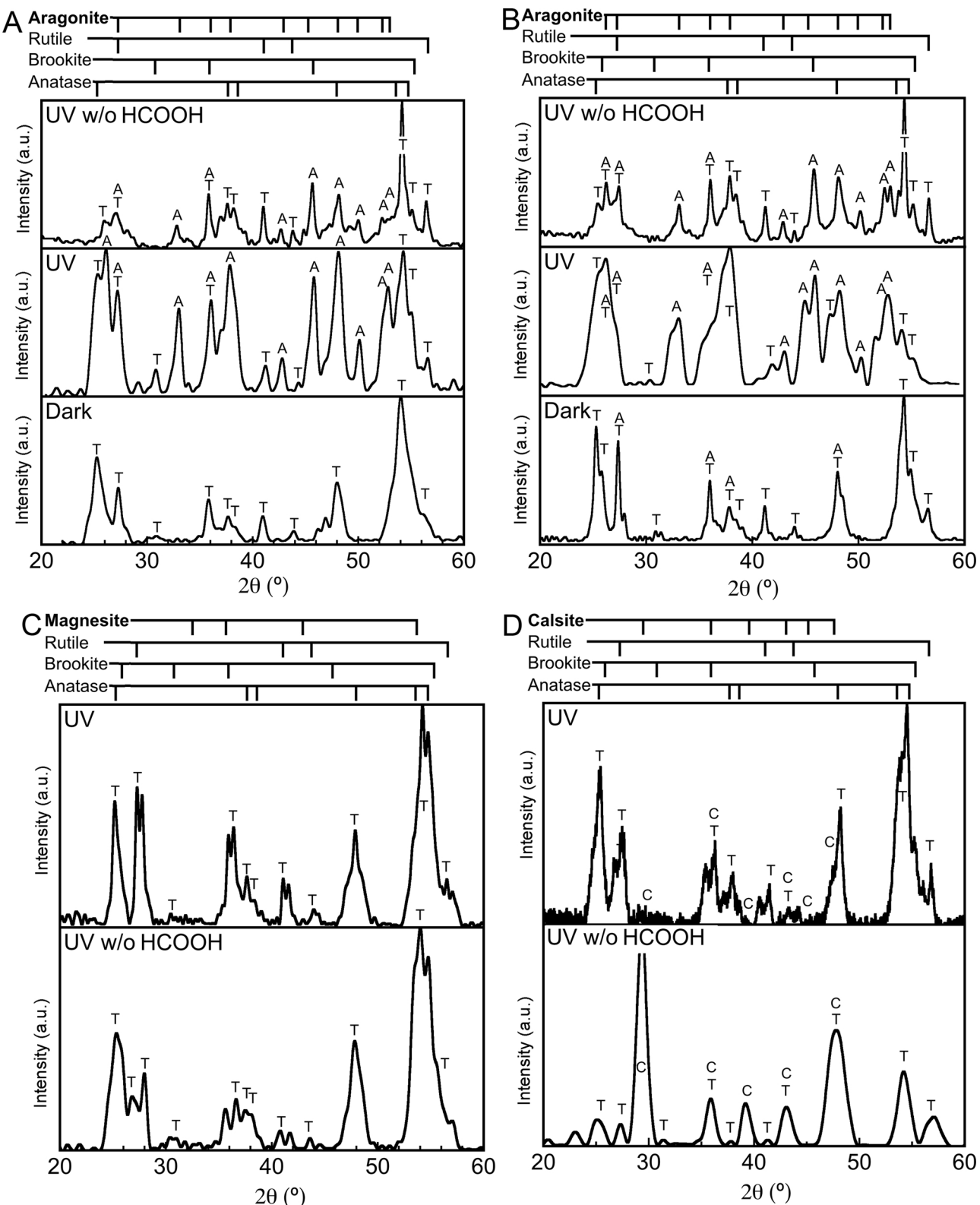


Fig. 8. X-ray diffraction spectra of PSF-01 surface after 15 experimental cycles without formic acid system under UV irradiation. [A] Evian, [B] Contrex, [C] Mg(HCO₃)₂ solution, and [D] Ca(HCO₃)₂ solution. “T” indicates anatase, brookite, or rutile crystal form of TiO₂, “A” indicates CaCO₃ aragonite, and “C” indicates CaCO₃ calcite.

(NaHCO₃, KHCO₃, Mg(HCO₃)₂, and Ca(HCO₃)₂) (Fig. 10). We observed that the photocatalytic degradation rate of formic acid was affected by the concentration of HCO₃⁻ irrespective of the counterion, and the photocatalytic activity was decreased with increasing HCO₃⁻

concentration. The decay curve of photocatalytic activity with increasing HCO₃⁻ concentration was fitted using the following equations:

$$K = 1.6 \times C^{-0.613} \quad (9)$$

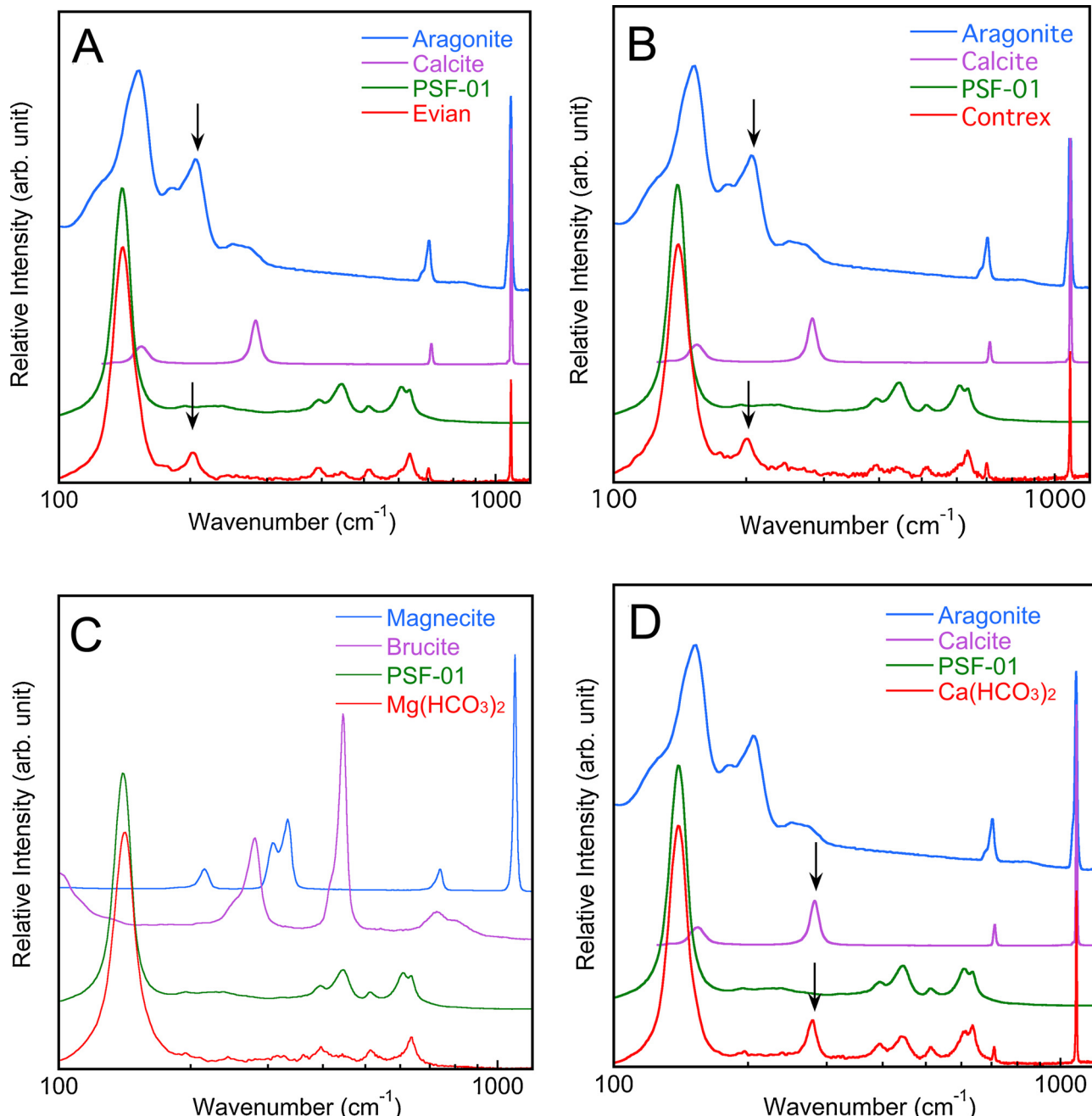
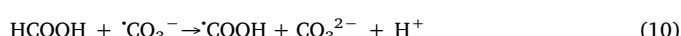


Fig. 9. Raman spectra of PSF-01 surface after 15 experimental cycles without formic acid system under UV irradiation. [A] Evian (arrows indicate characteristic peak of aragonite crystal form), [B] Contrex (arrows indicate characteristic peak of aragonite crystal form), [C] $\text{Mg}(\text{HCO}_3)_2$ solution, and [D] $\text{Ca}(\text{HCO}_3)_2$ solution (arrows indicate characteristic peak of calcite crystal form). Raman spectra of the crystal forms were obtained from the RRUFF database [19].

where K is the photocatalytic degradation rate (h^{-1}) of $1 \times 10^{-3} \text{ M}$ formic acid, and C is the concentration of HCO_3^- (mg/L). Under real-world conditions, factors such as UV light intensity and concentrations of contaminants would be added to this equation, however, it can be used simply to estimate the decrease in photocatalytic activity with increasing HCO_3^- concentration.

As shown in Figs. 6 and 8, the decrease in degradation rate of HCO_3^- was small in presence of formic acid, which could be attributed to the oxidation of formic acid during the photocatalytic oxidation of HCO_3^- as shown in (10).



The active species formed in Eq. (5), $\cdot\text{CO}_3^-$, oxidizes formic acid as shown in Eq. (10). This oxidation mechanism of organic compound by

$\cdot\text{CO}_3^-$ was described by Kumar et al. [13]. Then, $\cdot\text{COOH}$ in Eq. (10) is converted to CO_2 , as shown in Eq. (4). Direct reaction between $\cdot\text{OH}$ from Eq. (3) and $\cdot\text{COOH}$ from equation (4) occurs and conversion of HCO_3^- to CO_3^{2-} is inhibited. Thus, avoiding the oxidation of organic compound as per Eq. (10) could be the reason for the faster degradation rate of HCO_3^- and larger amount of CaCO_3 formation in absence of formic acid. Although inhibition of the reaction rate of formic acid oxidation with increasing concentration of HCO_3^- was observed not only in the presence of Ca^{2+} but also in the presence of other counterions (Fig. 10), however, a decrease in HCO_3^- concentration with photocatalysis was only observed in the presence of Ca^{2+} as shown in Figs. 6 and 8. This could be because in the photocatalytic reaction system, it is considered that CO_3^{2-} present in aqueous solutions with Na^+ , K^+ , Ca^{2+} and Mg^{2+} are formed from photocatalysis of HCO_3^- . In

Table 2

Elemental composition of the precipitate on the surface of the photocatalyst, as determined by energy dispersive X-ray spectrometry.

Elements	Evian		Contrex		(Atom %)
	Dark HCOOH	UV HCOOH	UV	Dark HCOOH	
C%	6.4	24.9	24.1	18.1	19.4
O%	58.3	55.2	58.5	51.7	57.4
Na%	0.0	0.1	0.1	0.0	0.1
Mg%	n.d.	0.0	0.0	n.d.	0.0
Al%	0.2	0.1	0.2	0.1	0.1
Si%	0.1	0.0	0.0	0.1	n.d.
S%	0.0	0.0	0.0	0.0	0.4
Ca%	0.2	15.1	16.6	22.1	22.0
Ti%	34.8	4.5	0.3	7.8	0.3
Sr%	n.d.	0.1	0.0	0.1	0.2
O%/C%	9	2	2	3	3
C%/Ca%	42	2	2	1	1
Ca%/Sr%	–	302	–	369	92
					98

HCOOH = formic acid.

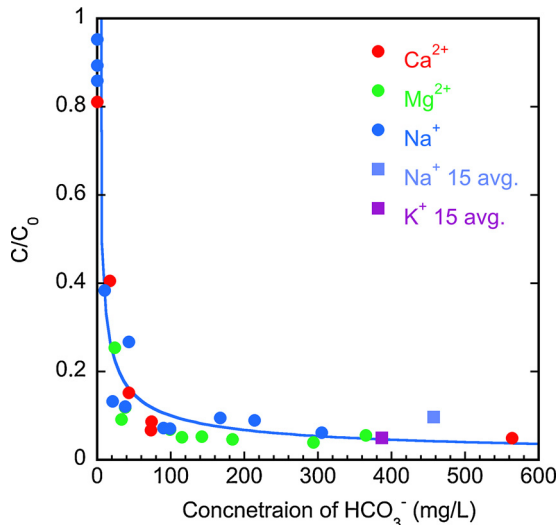


Fig. 10. Changes in the rate constant of photodegradation of formic acid with increasing HCO₃⁻ concentration when bicarbonate salt solutions containing the indicated counterions were circulated through the system. [●] Degradation rate of formic acid for one experimental cycle under UV irradiation, [■] average rate of degradation of formic acid for 15 experimental cycles under UV irradiation.

case of Ca²⁺ system, Ca²⁺ coordinates with CO₃²⁻ resulting in the formation of a precipitate, while carbonates of other cations were water soluble [25], and there is an immediate equilibrium between HCO₃⁻ and CO₃²⁻, which is more towards HCO₃⁻ [26,27]. As a result, decrease in HCO₃⁻ concentration was not observed after photocatalysis in spite of formation of CO₃²⁻, i.e., reaction between CO₃²⁻ and HCO₃⁻ did not occur in systems containing Na⁺, K⁺ and Mg²⁺.

With these results we can say that if photocatalysis-based processes are to be used to purify environmental water, combination of ion exchange filter is needed due to decrease in photocatalytic activity by HCO₃⁻ present in water. One of the drawback is the additional installation of the ion exchange cartridge for removing HCO₃⁻, which would increase the set-up and running costs making the implementation of the photocatalytic water purification system to developing countries difficult. Another limitation would be the accumulation of calcium carbonate on the photocatalytic system thereby blocking the flow channel. In this research work, since we have identified that the precipitate was a single species (calcium carbonate), it may be possible to use a simple maintenance procedure such as flushing with citric acid

to remove the precipitate from the photocatalytic system. Moreover, we have found that photocatalytic activity was affected by the concentration of HCO₃⁻, the size of the photocatalytic system can be tweaked, depending on the concentration of HCO₃⁻ in the source water, i.e., the size of photocatalytic water purification system will be increased inversely as per Eq. (9).

Furthermore, precipitation of metal silicates on a photocatalytic system also needs to be addressed. SiO₃²⁻ is a major component of groundwater, and in boilers CaSiO₃ precipitates from within the vessel when the source water includes SiO₃²⁻ together with Ca²⁺ [28]. Our photocatalytic system is different from a thermal system such as a boiler; however, before a commercial photocatalytic water purification system can be established, it is also important to probe the effect of silicate containing precipitates on photocatalysis [29].

4. Conclusion

Herein we examined which major inorganic components of groundwater influence the photocatalytic activity of a TiO₂ ceramic photocatalyst. We used Evian and Contrex as representative groundwater systems and four bicarbonate salt solutions containing Na⁺, K⁺, Mg²⁺, or Ca²⁺ as major components, as simulated groundwater systems. Degradation of formic acid was used as an index of photocatalytic activity. We found that HCO₃⁻ concentration affected the photocatalytic activity independently of which cation was present. When Evian, Contrex, or Ca(HCO₃)₂, were circulated through the photocatalytic water purification system for 15 experimental cycles of 8 h each, a precipitate accumulated on the surface of photocatalyst, which we identified as calcium carbonate. When Evian or Contrex were used, the crystal form of the calcium carbonate was aragonite, and when Ca(HCO₃)₂ was used, it was calcite. With these water systems, photocatalytic activity remained constant throughout the purification process despite the accumulation of the precipitate. This was because calcium carbonate does not absorb light in the UV-A region, which was the wavelength range used to excite the photocatalyst. Thus, for commercial photocatalytic water purification systems, the concentration of HCO₃⁻ in source water will dictate the size of the system, and acid cleaning will be needed to prevent blockage of the flow channel by depositing calcium bicarbonate on the photocatalyst.

Acknowledgement

This research work was carried out by the internal budget of our institute.

Appendix A. Supplementary data

Supplementary material related to this article can be found, in the online version, at doi:<https://doi.org/10.1016/j.apcatb.2018.10.022>.

References

- [1] A. Kouzayha, A.A. Ashi, R.A. Akoum, M.A. Iskandarani, H. Budzinski, F. Jaber, Bull. Environ. Contam. Toxicol. 91 (2013) 503–509.
- [2] D. Mondal, B. Ganguli, S.S. Roy, B. Halder, N. Banerjee, M. Banerjee, M. Samanta, A.K. Giri, D.A. Polya, Water 6 (2014) 1100–1117.
- [3] V. Lekskulchai, ScienceAsia 41 (2015) 409–413.
- [4] A. Ender, N. Goeppert, F. Grimmeisen, N. Goldscheider, Sci. Total Environ. 15 (2017) 996–1106.
- [5] N.K. Leite, J. Stolberg, S.P. Cruz, A.O. Tavela, J.L. Safanelli, H.R. Marchini, R. Exterkoetter, G.M.C. Leite, A.V. Krusche, M.S. Johnson, Environ. Earth Sci. 77 (2018) 77–80.
- [6] J.O. Odiyo, R. Makungo, Int. J. Environ. Res. Public Health 15 (2018) 317–329.
- [7] J.M. Kayembe, F. Thevenon, A. Laffite, P. Sivalingam, P. Ngelinkoto, C.K. Mulaji, J.-P. Otamonga, J.I. Mubedi, J. Poté, Int. J. Hygiene Environ. Health 221 (2018) 400–408.
- [8] Photocatalysis Industry Association of Japan, http://www.piaj.gr.jp/piaj_product/list.html.
- [9] M. Hayashi, T. Ochiai, S. Tago, H. Tarayama, T. Hosoya, T. Yahagi, A. Fujishima, Catalysts 7 (2017) 158–167.

[10] P.J. Sullivan, F.J. Agardy, J.J. Clark, *The Environmental Science of Drinking Water*, Elsevier Butterworth-Heinemann, Oxford, 2005.

[11] R.A. Freeze, J.A. Cherry, *Groundwater*, Prentice-Hall Inc., New Jersey, 1979 pp. 85.

[12] C. Guillard, E. Puzenat, H. Lachheb, A. Houas, J.-M. Herrmann, *Int. J. Photoenergy* 7 (2005) 1–9.

[13] A. Kumar, N. Mathur, J. Colloid Interface Sci. 300 (2006) 244–252.

[14] A. Lair, C. Ferronato, J.-M. Chovelon, J.-M. Herrmann, *J. Photochem. Photobiol. A: Chem.* 193 (2008) 0193–203.

[15] J. Jiang, C. Chen, B. Xiao, Z. Bai, C. Jiang, C. Yamg, Y. Wu, X. Wang, *Cryst. Eng. Comm.* 19 (2017) 7332–7338.

[16] T. Mishima, S. Ohsawa, M. Yamada, K. Kitaoka, *Jpn. Assoc. Hydrol. Sci.* 4 (2009) 157–168.

[17] T. Liu, Q. Li, Y. Xin, Z. Zhang, X. Tang, L. Zheng, P. Gao, *Appl. Catal. B: Environ.* 232 (2018) 108–116.

[18] G.V. Buxton, C.L. Greenstock, W.O. Helman, A.B. Ross, *J. Phys. Chem. Ref. Data* 17 (1988) 513–886.

[19] H. Wang, C. You, Z. Tan, *Chem. Eng. J.* 350 (2018) 89–99.

[20] C.H. Saylor, *J. Phys. Chem.* 32 (1928) 1441–1460.

[21] J.L. Wray, F. Daniels, *J. Am. Chem. Soc.* 79 (1957) 2031–2034.

[22] [Dataset] RRUFFTM database: <http://rruff.info>.

[23] H. Selcuk, *Water. Res.* 44 (2010) 3966–3972.

[24] A. Lair, C. Ferronato, J.-M. Chovelon, J.-M. Herrmann, *J. Photochem. Photobiol. A: Chem.* 193 (2008) 193–203.

[25] G.M. Marion, *Geochim. Cosmochim. Acta* 65 (2001) 1883–1896.

[26] W.W. Rudolph, G. Irmer, E. Königsberger, *Dalton Trans.* (2008) 900–908.

[27] M. Legarra, A. Blitz, Z. Czégény, M.J. Antal, *Ind. Eng. Chem. Res.* 52 (2013) 13241–13251.

[28] Y. Xu, B. Dong, X. Dai, *Desalination* 361 (2015) 38–45.

[29] L.Z. Lakshtanov, S.L.S. Stripp, *Geochim. Cosmochim. Acta* 74 (2010) 2655–2664.